ELSEVIER

Catalysis Today 47 (1999) 51–71

CATALYSIS TODAY

New technology for production of spherical alumina supports for fluidized bed combustion

Z.R. Ismagilov*, R.A. Shkrabina, N.A. Koryabkina

Boreskov Institute of Catalysis, Pr.Ak.Lavrentieva, 5, Novosibirsk 630090, Russian Federation

Abstract

Fluidized bed catalytic combustion has proved to be very promising for industrial application. The milestone problem is the development of support and catalyst with a high mechanical and thermal stability. We have developed a new technology for production of alumina supports with desired spherical shape, texture and structure. In this paper several pathways to produce aluminum hydroxide of a pseudoboehmite structure including conventional and new technologies are discussed. Properties of spherical granules depend on the method of granulation and most attention has been paid to development and optimization of hydrocarbon–ammonia molding to produce uniform alumina spheres. Several methods to estimate mechanical strength of spherical aluminas are applied to evaluate mechanical durability of prepared catalysts in a fluidized bed. Optimization of high quality spheres production focused on study of the effect of initial hydroxide properties and molding conditions on properties of the final product. Modification of spherical alumina with oxides of Mg, Ce, La and Si proved to be effective to substantially improve the mechanical and thermal stability. This effect is most pronounced when pairs of these dopes are introduced simultaneously.

Keywords: Aluminum hydroxide; Pseudoboehmite; Gibbsite amorphization; Spherical alumina; Fluidized bed; Granulation; Hydrocarbon–ammonia molding; Mechanical strength; Thermal stability; Modification by Mg, La, Ce, Si; Double modification

1. Introduction

It is known [1–6] that the properties of the initial hydroxide determine not only the type of aluminas, but also their thermal stability. One should consider this fact when choosing an appropriate oxide as a catalyst support. The transformation routes show that χ-Al_2O_3 exhibits the lowest thermal stability. The most widely used industrial support is γ-Al_2O_3 obtained from pseudoboehmite because:

- it is quite easy to control its properties at the preparation stages;
- this hydroxide can react with acids yielding pastes suitable for molding.

Below we shall concentrate in more detail on the problems in the production of pseudoboehmite and γ-Al_2O_3 with desired properties.

Catalytic oxidation, including the catalytic combustion of fuels, is one of the main directions of R & D at the Institute of Catalysis. Combustion of fuel–air mixtures that are close to stoichiometry is a highly exothermic process, and we proposed to use fluidized

*Corresponding author.

0920-5861/99/$ – see front matter
PII: S0920-5861(98)00283-1

bed catalytic reactors [7–10], the so-called catalytic heat generators (CHGs).

Besides, CHG used for the fuel combustion imposes severe demands on the catalyst, which should retain its activity and resistance to attrition in the fluidized bed where local thermal shocks occur. Apparently, the properties of the catalyst are determined by those of the support (its mechanical strength and thermal stability). We have formulated the following demands on the catalysts and supports to be used in the process [10–12]:

- Support granules should have a regular spherical shape and be 1–3 mm in size with a narrow particle size distribution (1.0–1.4, 1.6–2.0, 2.0–2.5 mm, etc.) to avoid catalyst losses due to mechanical attrition and uptake caused by the non-uniform particle size distribution.
- Support and catalyst granules should be strong enough to avoid cracking during the operation. The average strength of spherical granules should not be less than 18 MPa.
- Support (and catalyst) should retain their key properties during the operation when local overheating up to 1000°C occurs on the catalyst granules.

Taking all these requirements into account [10,12] we have concentrated on the development of spherical supports for CHG catalysts on the basis of γ-Al_2O_3.

2. Pathways to produce aluminum hydroxide of a pseudoboehmite structure

It is known [1–6] that γ-alumina is the dehydration product of aluminum monohydrate with a boehmite or pseudoboehmite structure. Pseudoboehmite differs from boehmite by having additional water molecules inserted into the interlayer space roughening the structure [1]. Monohydrate with primary particles smaller than 250 Å is a highly dispersed and chemically active hydroxide. It has a higher specific surface area and can produce soluble basic salts in the reaction with acids. These salts serve as good binders in molding [13]. That is why this highly dispersed hydroxide is used to produce granular γ-Al_2O_3 with desired properties.

2.1. Conventional technologies

A periodic precipitation from solutions of sodium aluminate with acids or from solutions of aluminum salts (nitrates, sulfates) with an alkali (NaOH, NH_4OH) is the most industrially recognized method for synthesis of pseudoboehmite aluminum hydroxide. In both cases gibbsite is used as a raw material to prepare the solutions of aluminum compounds. Precipitation conditions (pH, temperature), time and temperature of precipitate aging and other process parameters determine the properties of hydroxide, such as porous structure (at 110°C), dispersity, arrangement of primary particles in secondary aggregates, etc.

Detailed information about the conventional procedure of pseudoboehmite synthesis is given in [1,14].

Regarding the precipitation temperature, we distinguish the so-called "cold" (about 20°C) and "hot" (about 100°C) precipitation. It will be shown below that the properties of pseudoboehmite hydroxides obtained via the cold and hot precipitation are substantially different. That is why the so-called "mixed" pseudoboehmite hydroxides are used in the industry. The hydroxides of the cold and hot precipitation are mixed usually in a ratio of 1:3 to provide better filtering and washing from impurities.

Recently, continuous precipitation methods have been developed. In this case precipitation is conducted in a single flow at 40–50°C followed by aging at 30–35°C [15].

2.2. New technologies

Pseudoboehmite synthesis via gibbsite amorphization and processing has recently become quite popular. There are many amorphization procedures, such as mechanical or mechano-chemical activation [16,17]; pulse heating in a flow of flue gases [18], in a hot air flow [19], or in the fluidized catalyst bed where the heat for amorphization is supplied by catalytic fuel combustion [7–12]. Further processing of this amorphous product yields hydroxide of the pseudoboehmite type.

The process of gibbsite amorphization in CHGs has been developed at BIC and commercialized in Russia [6,7,12]. Fig. 1 shows a schematic view of a CHG. In this reactor heating of powdered gibbsite occurs with a

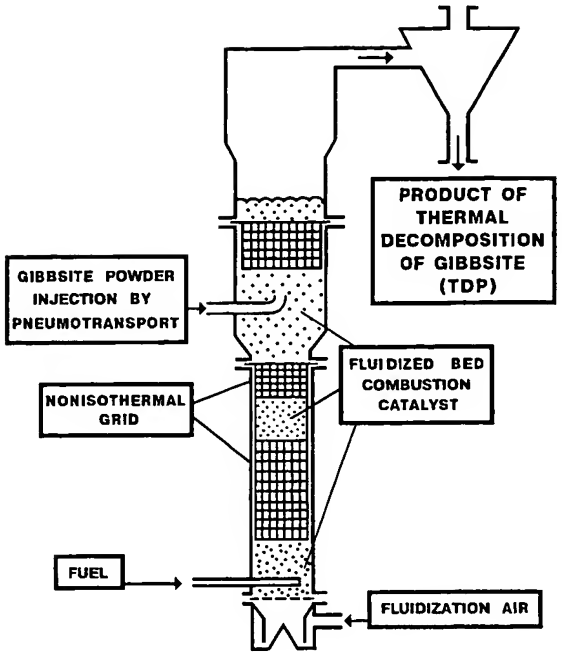

Fig. 1. Scheme of catalytic heat generator for thermal decomposition of gibbsite.

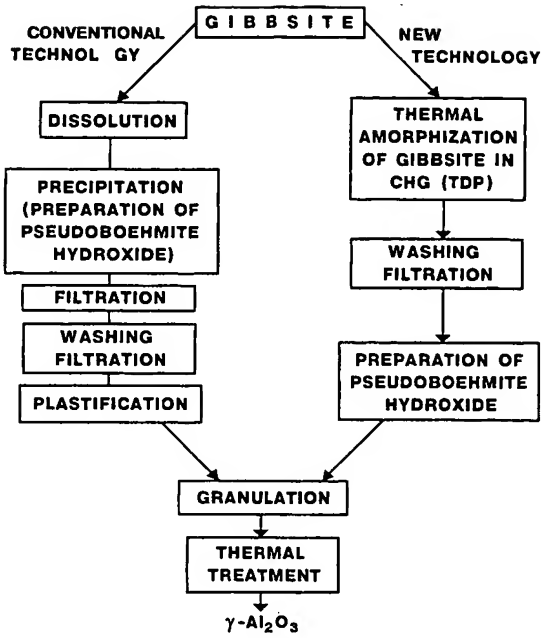

Fig. 2. Scheme of preparation of γ-Al_2O_3.

very short residence time (less then 0.1 s), and gibbsite amorphization occurs simultaneously with its dehydration.

The resulting thermal decomposition product (TDP) of gibbsite has a higher reactivity. It allows us to produce pseudoboehmite hydroxide avoiding conventional stages of gibbsite dissolving and reprecipitation.

Table 1 shows the TDP properties as compared to those of the initial gibbsite.

Pseudoboehmite formation from TDP occurs at 110–120°C in acidic medium (pH~3–4) as described elsewhere [6,20,21]. The pseudoboehmite content in the final product attains 80–90%, while its dispersity (estimated by the coherent dissipation region, c.d.r.) does not exceed 100 Å.

Fig. 2 is a schematic representation of the pseudoboehmite hydroxide production according to the new CHG technology as compared with the traditional procedure.

Table 1
Main properties of thermal decomposition product (TDP)

Product	S_{BET} (m^2/g) (110°C)	Water content (wt%)	Chemical activity[a] (wt%)
Gibbsite	<1	34	~8
TDP	250	10–13	85

[a]Chemical activity is determined as the amount of Al^{3+} ions transferred to the solution under dissolution in 5 N NaOH at 60°C as described in [6].

2.3. *Properties of pseudoboehmite aluminum hydroxide*

A variety of methods used for the pseudoboehmite hydroxide production leads to different properties of solids which are compared in Table 2.

Note that the morphology of the pseudoboehmite is also different. TEM was used to study the packing of the primary particles into secondary aggregates and the morphology of samples 1–3 [22–24].

Sample 4 obtained via salt precipitation consisted of the roughly packed secondary aggregates formed by fibers made of thin (~40 Å) needles.

Pseudoboehmite produced by continuous precipitation (sample 5) was an assembly of small needles 20–30 Å closely packed in fibers ~15 000 Å long. Large

Table 2
Effect of preparation conditions on the properties of pseudoboehmite hydroxide

Preparation procedure	Preparation conditions		H_2O content (wt%)	S_{BET} (m^2/g)	Primary particle size (Å)	Pore volume (cm^3/g) (radius, r, Å)		
	pH	t (°C)				V_Σ	<40	40–1000
(1) Reprecipitation (cold precipitation)	8.5	20	85	270	~30	0.572	0.322	0.075 (>1000, 0.175)
(2) Reprecipitation (hot precipitation)	8.5	100	59	110	150–180	0.945	0.125	0.235 (>1000, 0.585)
(3) Mixed hydroxide (cold:hot=1:1)	–	–	75	220	50, 150	0.460	0.270	0.190
(4) Acid precipitation	7	70	81	290	~40, 120	1.410	0.210	0.790 (>1000, 0.410)
(5) Continuous precipitation	8.5	40	80	250	30–40	0.314	0.154	0.058 (>1000, 0.102)
(6) Gibbsite thermal decomposition in CHG	3–4	130	75	200	50, 150	0.480	0.270	0.210

shapeless aggregates were scarce (unlike in sample 1). Therefore, morphologically this type of pseudoboehmite is similar to the ordinary one containing needles packed in fibers [1].

Pseudoboehmite produced from TDP (sample 6) was similar by its morphology to that produced by the mixed precipitation method (sample 3). It consisted of needles and almost spherical particles packed in large aggregates as plates larger than 1000 Å.

3. Preparation of spherical granules and methods of property control

3.1. Methods of granulation

Fig. 3 presents the methods used to produce spherical granules and shows the size of granules produced by each method. Let us consider the peculiarities of different granulation methods.

3.1.1. Rotating pan granulation

A round rotating dish is one of the best known methods to produce spherical granules [25–27]. Oxide or hydroxide powders in the presence of water or binding solutions are fed into the dish and the small rotating particles develop layer by layer into larger spherical granules. Rotation of wet extrudates, whose height and diameter are approximately the same, is also used to produce spherical shape of granules. The latter method does not allow one to produce a narrow particle size distribution, and the particle diameter is as a rule larger than 2 mm. Besides, the strength of the alumina granules does not exceed 10 MPa. These disadvantages make it impossible to use such granules in a moving or fluidized bed.

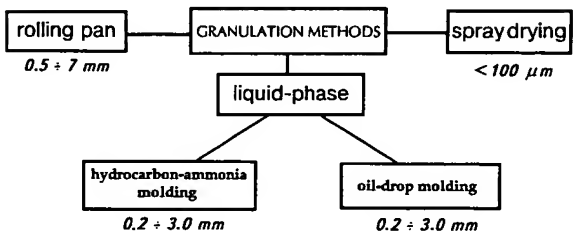

Fig. 3. Granulation methods of spherical alumina production.

3.1.2. Gas phase granulation (spray drying)

This method is a suitable technique to produce microspherical particles not exceeding 0.1 mm. In a spray dryer a hydrogel or a sol (solid content less than 20 wt% [25]) is sprayed through nozzles into a heated zone. Catalytic cracking in moving beds is an example of a process involving a catalyst produced by this procedure. However, these microspherical granules can hardly be used in the fuel combustion at high linear flow rates.

3.1.3. Liquid-phase molding

In this method special die plates with cylindrical holes are used to produce drops of an aluminum hydroxide sol, which then gets into an oil layer at the top of the column and thus assumes a spherical shape due to the surface tension. Further on, these granules congeal during their moving down through the gelating media layer (gel-formation). Two technologies are distinguished depending on the congealing conditions: oil and hydrocarbon–ammonia molding.

3.1.4. Oil molding

In this case a spherically shaped sol (containing, e.g., hexamethylenetetramine (HMTA) [28] or an organic monomer [29] is introduced into a hot oil (~90°C) [27]. Congealing of the sol occurs either by means of neutralization with ammonia or due to HMTA decomposition (or monomer polymerization). The method provides formation of uniform spherical granules. But the use of the hot oil and the necessity to keep the sol drops for quite a long time (>10 min) under such severe conditions to complete the HMTA decomposition or the polymerization are obvious drawbacks.

3.1.5. Hydrocarbon–ammonia molding

The sequence of main stages and a principal schematic view of the hydrocarbon–ammonia molding (HAM) [30,31] is represented in Figs. 4 and 5.

Aluminum hydroxide is treated by an acid-peptizer to obtain a flowing (plastic) sol. Then the sol drops through a die plate into the liquid hydrocarbon layer on top of the molding column, where it assumes a spherical shape due to the surface tension. Further on, spherical sol granules move down into the ammonia solution. The sol transforms to a gel in the coagulant

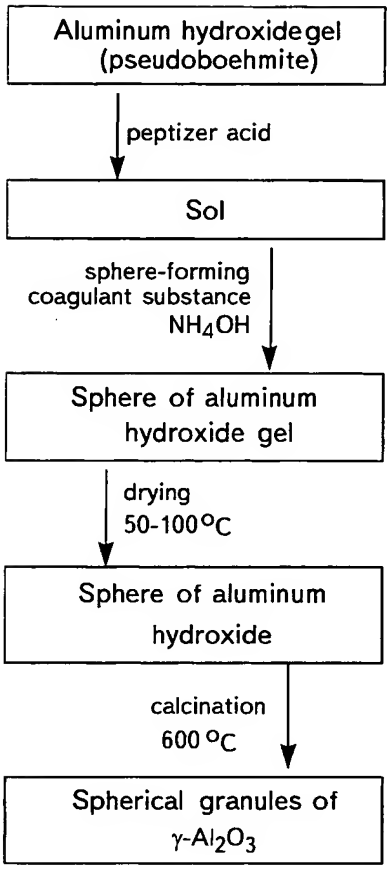

Fig. 4. The main stages of the hydrocarbon–ammonia molding.

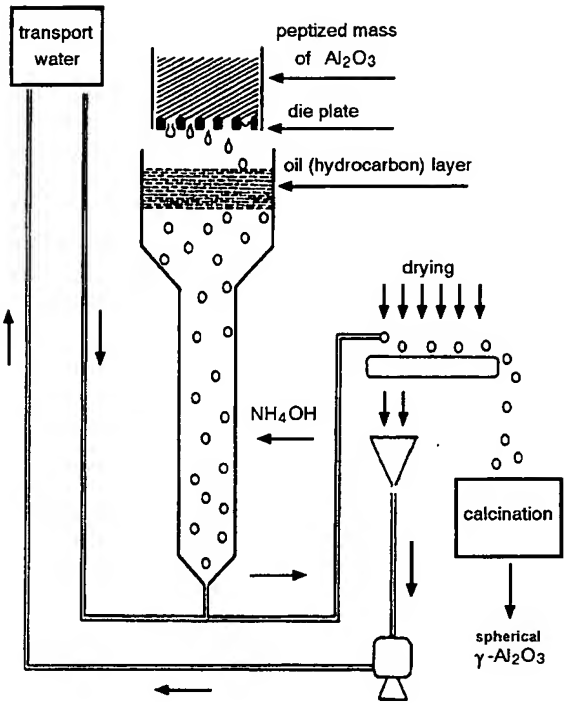

Fig. 5. Principal scheme of the hydrocarbon–ammonia molding technology.

media, and thus granules are congealed. Then the spherical granules of the gel are dried and calcined to produce spherical alumina.

The main physical and chemical processes occurring during all the molding stages, and the effects of technological parameters on the properties of the final spherical alumina bodies are discussed in [7,22–24,30–33].

Colloidal processes occurring at the plasticizing stage, namely how the pseudoboehmite morphology (degree of aggregation) and the amount of acid affect the texture of both hydroxide and spherical alumina, were studied in [23,24,30–33]. Only the hydroxide with contacts due to coagulation between the primary particles appears to disaggregate in the acid. No disaggregation occurs in the hydroxides with contacts due to crystallization. Contacts between the primary particles in the hot-precipitation pseudoboehmite (sample 2, Table 2) belong to the crystallization type due to chemical interactions, and this hydroxide cannot be peptized by acid to produce the sol for HAM [30–33]. In the cold and continuous precipitation hydroxides (samples 1 and 5, Table 2, respectively), the primary particles are bound by electrostatic or van der Waals forces. Both types of contacts are present in the mixed (sample 3, Table 2), acid-precipitation or TDP-originated hydroxides (samples 4 and 6, Table 2, respectively). Therefore, these hydroxides can be used to produce a plastic mass by acid treatment.

The stage of the sphere formation includes two steps:

- spherical granules formation in a hydrophobic medium of a liquid hydrocarbon layer by means of surface tension;
- congealing of the spheres.

There is an optimal height of the hydrophobic liquid layer because the residence time affects the shape and uniformity of granules. The residence time in the coagulant – NH_4OH solution, its concentration and

temperature influence the rate of coagulation; the uniformity of coagulant diffusion into the granule also affects the properties of the spherical alumina produced [30].

The porous structure of the hydroxide, and thus of the resulting alumina, has been shown to depend on the properties of the initial hydroxide. Thus, with the cold-precipitation samples (sample 1, Table 2) the sol formed during peptization looses its macropores, since the large secondary aggregates decompose. The gel after coagulation also does not contain macropores, and therefore, the spatial arrangement of coagulation contacts in the gel is not uniform enough.

The porous structure of the mixed-precipitation hydroxides at the stages of peptization–coagulation depends on the ratio between cold- and hot-precipitation hydroxides in the mixed precipitate. The higher the contribution of the hot-precipitation hydroxide, the less are the changes in the porous structure during peptization–coagulation [23]. Thus the volume of mesopores (300–1000 Å) in samples 3 (Table 2) changed insignificantly.

Samples 5 and 6 (Table 2) had the same behavior during the coagulation process as their analogs in morphology (samples 1 and 3).

In general, HAM allows one to produce spherical γ-Al_2O_3 granules from the aluminum hydroxide of pseudoboehmite structure containing coagulation contacts between the primary particles. But the properties of γ-Al_2O_3, e.g. mechanical strength, and thermal stability, depend on the morphology and the pore structure of the initial hydroxide.

3.2. *Methods to estimate the mechanical strength of granules*

A high mechanical strength is one of the demands on γ-Al_2O_3-supported catalysts for CHG equipment with the fluidized catalyst bed. There is a variety of methods to determine this key parameter and it is important to choose the most appropriate method, which adequately reflects the mechanical impact on the spherical granules in the fluidized bed of the CHG apparatuses.

Apparently, the term "mechanical strength" includes different characteristics, such as resistance to crushing and to attrition, resistance to thermal and mechanical shock, etc.

As regards testing procedures, static and dynamic methods are used [34,35]. Methods determining the crushing strength of individual granules between two parallel plates belong to the first type. Attrition and impact loads are usually tested under dynamic conditions.

Taking into account results obtained earlier [35–40], we used the following strength measurements:

- crushing strength;
- attrition strength;
- impact strength.

Fig. 6 shows schematically mechanical stresses on granules in the methods we used to determine the mechanical strength.

Sample strength according to the first method (P, MPa) was calculated as the arithmetic mean from values determined for 30 granules. The minimum and maximum sample strengths were determined as the arithmetic mean for five granules possessing the minimum (P_{min}) or maximum (P_{max}) strength. Since the granules of minimum strength were the first to be crushed, it was important to fix this particular parameter, P_{min}.

Attrition strength determined by the second method was characterized by two attrition rates: V_1 (%/min) at

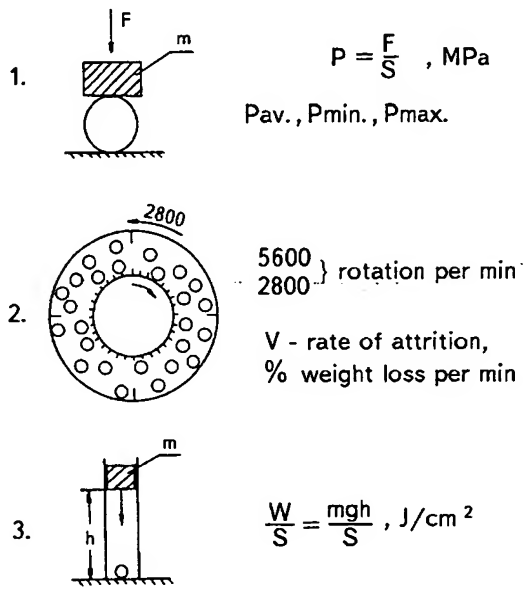

Fig. 6. Basic schemes of mechanical testing.

the initial part, and V_2 (%/min) over the stationary part of the kinetic curve in the coordinates "attrition (%)-versus-time (min)" at fixed attrition degrees (15% or 30%). We adjusted the process so that no crushing of granules occurred.

Impact strength was measured under multiple loads on each granule in a chosen set of 50 pieces to complete crushing at a constant energy $W_o=mgh$, where m is the mass of the load falling from height (h). The number of cycles (impacts), K, before crushing of the granule and the number of granules (n) crushed after K impacts were fixed.

Granules of crushing strength below 10 MPa failed to resist loads under the attrition conditions chosen, they crushed during testing. Samples with an average crushing strength over 10 MPa were undergoing pure attrition, its rate being practically constant and equal to 0.22%/min. No crushing is observed and an important demand is formulated: the mechanical strength of granules should exceed 10 MPa to avoid crushing under dynamic conditions.

We used the third method in order to study the impact strength.

Fig. 7 shows the kinetic energy providing a 50% crush of the granules (W_{sp}, J/cm^2) versus crushing strength (MPa). Apparently, the impact strength is proportional to the crushing strength. Therefore, the stronger the granule under static test conditions (P_{av}), the less fragile it is.

Such a W_{sp}-versus-P_{av} function is true for aluminas independent of their phase composition. However, we found that δ- and α-Al_2O_3 were more fragile at the same P_{av} than γ-Al_2O_3 (Fig. 8).

The above results show that the stronger the individual granules according to the static method, the better they resist attrition and impact.

3.3. *Effect of initial hydroxide properties on the mechanical strength of the support*

In this section results on the mechanical strength of spherical γ-Al_2O_3 obtained from the pseudoboehmite hydroxides synthesized via various methods will be discussed.

Table 3 presents the main properties of spherical γ-Al_2O_3 obtained from the pseudoboehmites described in Table 2. The numbering of samples corresponds to that of Table 2. Note that as it is not possible to obtain spherical γ-Al_2O_3 via HAM from the hot-precipitation hydroxide (sample 2, Table 2), there are no data for γ-Al_2O_3 from this hydroxide. Pseudoboehmite synthesis from TDP has been described elsewhere [6,7].

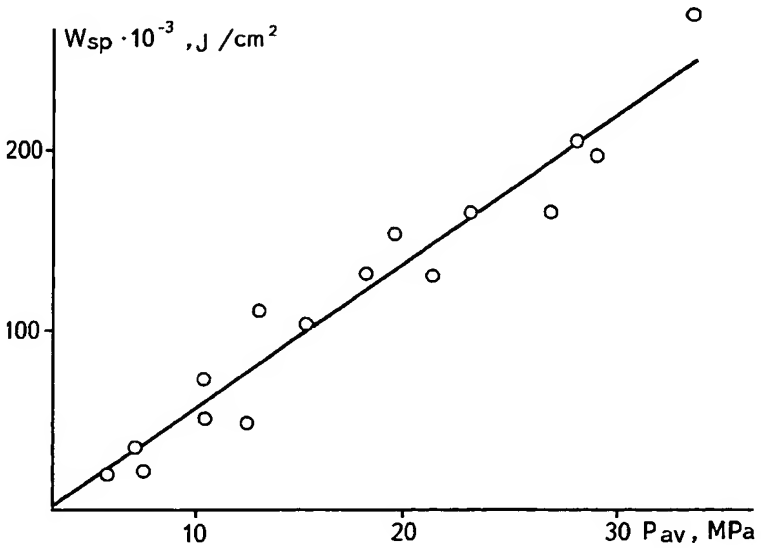

Fig. 7. Critical specific kinetic energy W_{sp} as a function of P_{av}.

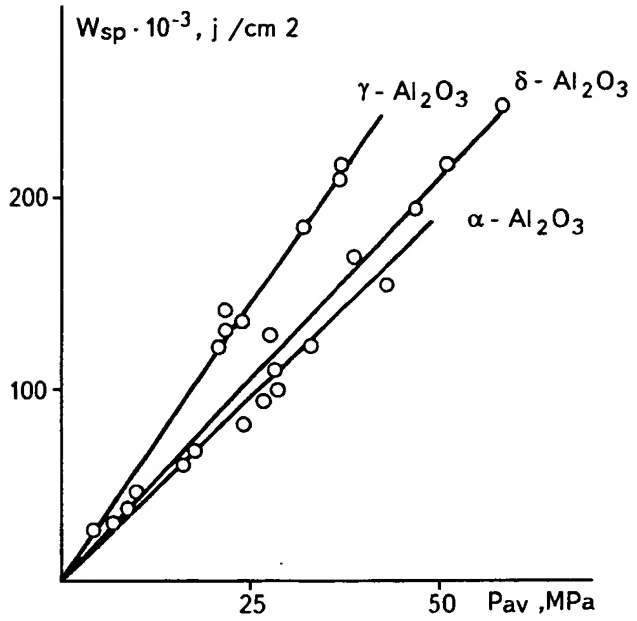

Fig. 8. W_{sp}- versus-P_{av} for various modifications of alumina.

Table 3 shows that the porous structure and the mechanical strength of the γ-Al_2O_3 are determined by the properties of the parent hydroxide.

Therefore, the character of contacts between the primary particles in aluminum hydroxide of the pseudoboehmite structure not only plays a key role in HAM, but also affects the structure and mechanical properties of γ-Al_2O_3.

The question rises whether one can change the character of the contacts in the aluminum hydroxide with the aim of further use for HAM.

Dispersing is a well known way to change the crystal structure and energy states of solids. Mechanical activation may improve the solid reactivity [41]: surface properties change, partial amorphization occurs, solubility improves, etc. All these processes do not depend on the changes of the particle size.

The influence of the milling intensity on the texture of reprecipitated aluminum hydroxides (AHs), on their properties and on the properties of the resulting Al_2O_3 is reported in [33]. It has been shown that mechanical activation resulted in crushing of the initial aggregates and some changes in the character of binding between the primary particles. So secondary aggregates decomposed by rupture of bonds between primary particles during the peptization

Table 3
Properties of spherical γ-Al_2O_3 (granule diameter 2–3 mm)

No.	Bulk density (g/cm^3)	S_{BET} (m^2/g)	V_Σ (cm^3/g)	Volume of pores with radius (r, Å) (cm^3/g)				Mechanical strength P (MPa)		
				40–100	100–1000	1000–10 000	>10 000	P_{av}	P_{max}	P_{min}
1	0.86	290	0.40	0.39	0.01	–	–	21	25	14
3	0.67	240	0.44	0.18	0.05	0.21	–	8	9	5
4	0.39	280	1.59	0.78	0.35	0.098	0.37	7	8	5
5	0.75	250	0.36	0.35	0.01	–	–	20	22	16
6	0.51	230	0.63	0.41	0.22	–	7	9	6	
7 (after grind. hydr.)	0.81	230	0.34	0.35	–	–	–	25	46	15
8 (from milled TDP)	0.80	225	0.40	0.40	–	–	–	24	42	14

stage. Increasing the milling intensity above the optimal magnitude resulted in a decrease of the specific surface and the total volume of pores (V_Σ) and the volume of pores with $r>1000$ Å. At a very high milling intensity the excess surface energy accumulated and the particles once again started to aggregate spontaneously, their surface and volume becoming partially inaccessible for the measurements.

TEM and X-ray spectroscopy evidenced the profound changes of the hydroxide structure with mild influence on the granulometry of the hydroxide powder. Therefore, mainly strong crystallization contacts between the particles are changed to weak coagulation contacts during disaggregation induced by mechanical activation. Using the AH milling, one can change the character of the contacts and thus affect the mechanical strength of γ-Al_2O_3 granules. Table 3 presents the properties of γ-Al_2O_3 (sample 7) obtained from the milled AH with mixed contacts between the secondary aggregates (sample 3, Table 2) [33]. In the case of spherical γ-Al_2O_3 preparation from the milled TDP (sample 8) the milling reduced the polydispersity of the TDP fractional composition to a minimum and increased its chemical activity thus reducing the optimal autoclave operation time and acid consumption. As in the case of reprecipitated hydroxide, we obtained a strong alumina with a monodisperse structure.

Using the approach suggested in [42,43], one can estimate the possible strength of a perfectly structured granule. According to very approximate estimates, P should exceed 100 MPa for a granule 1–3 mm in diameter. Such essential differences between the real and calculated strength values can be explained by large (micron scale) defects.

Inner cavities and cracks can be attributed to the macrodefects. A mosaic structure forming when the granule consists of separate weakly bound fragments is a defect as well. The size of defects and their disposition in the granule affect its strength essentially. X-ray analysis was used to study the defectness of granules with regard to their mechanical strength [44–46]. Curves of the Al K_α irradiation intensity with oscillations typical for each sample were obtained for the inner cuts of granules.

Scanning of weaker samples showed that the irradiation intensity oscillated intensively indicating numerous defects and microcracks which reduced the granule strength. The higher the strength the smaller the amplitude of the intensity oscillations.

3.4. *Influence of molding conditions on the mechanical strength*

The type of initial hydroxide and its ability to disaggregate in acids determines the specific surface, the porous structure and the strength of the γ-Al_2O_3 granules. Meanwhile, molding in the hydrocarbon liquid as well as granule solidification in the coagulant solution mostly affect the defectness of the shape, the inner cavities, the tensions and the other factors that essentially determine the granule strength.

It has been shown in [30] that the range of the interaction of the plastic sol (PS) with the coagulant (NH_4OH solution) depends on its concentration and the time of the granule stay in ammonia. In the same paper one can find the data on how the PS aging time, acid module, acid type and hydrocarbon layer height influence the mechanical strength, the shape and the fractional composition of the granule. The effects of the Al_2O_3 concentration in the PS, the ammonia solution and the PS temperatures have also been studied. The water amount in the plastic sol appears to have a less drastic effect than the ratio of capillary compression and skeleton rigidity. In the systems with weak skeletons (poorly crystallized or mechanically activated AH), capillary forces provide dense and strong γ-Al_2O_3 granules even if comparatively large amounts of water are removed. On the contrary, in the systems with rigid skeletons (roughly disperse AH) the macropores resist drying and calcination resulting in a decrease of the granule strength.

3.5. *Thermal stability and its estimation*

γ-Al_2O_3 is the most thermally stable alumina [1], since its transition to α-Al_2O_3 starts at the highest temperature. χ-Al_2O_3 is the least stable. Note that for all low-temperature aluminas transition to α-Al_2O_3 completes at 1200°C independent of their properties. According to Saalfeld [47], χ-Al_2O_3 has the most disordered structure characterized by various occupations of the Al^{3+} vacancies in the oxygen lattice. This factor determines the low thermal stability of this particular alumina, since Al^{3+} diffusion from the tetrahedral vacancies into the octahedral ones is easier

as the rhombic lattice of κ-Al_2O_3 is deformed. It is known [1] that in the low-temperature aluminas Al^{3+} occupies tetrahedral and octahedral vacancies, whereas in α-Al_2O_3 it occupies only the octahedral ones. Therefore, transition of aluminas into α-Al_2O_3 involves Al^{3+} diffusion into the octahedral vacancies and is accompanied by lattice rearrangements.

At present, there are many methods to produce γ-Al_2O_3-based spherical supports. Principal and technological adjustments yield supports possessing different properties (phase composition in particular). In [48], for instance, γ-Al_2O_3-based supports with various contents of χ-Al_2O_3 were studied at different calcination temperatures. Let us consider these results in more detail.

Fig. 9 shows how the crushing strength depends on the χ-Al_2O_3 content in the initial alumina (550°C) during its calcination. Apparently, the strength of spherical granules decreases during the calcination. The lowest strength was observed after thermal treatment at 900–1100°C independent of the alumina type. The crushing strength, P_{av}, starts to increase at 1200°C when the transition to α-Al_2O_3 completes, and bulk sintering sets on.

We can explain the decrease of the granule strength in the above temperature range in the following way. It is known that the transition to the high-temperature oxides, like δ-, κ-, and θ-Al_2O_3, causes a 2–3-fold increase of the primary particle size. Thus the radii of pores also increase at almost the same pore volume [49]. Sintering occurs by a surface diffusion mechanism, when particles stick together, but their centers do not approach each other (no porosity decrease, no shrinkage).

As a result, the number of contacts between the elementary particles imposed to mechanical tensions drops [40], and the strength of the whole granule also decreases. If this process is complicated by different rates of phase transitions and by change of structural parameters (as indeed occurs in the (γ+χ)-Al_2O_3 system), it is quite natural to expect drastic changes of mechanical properties. As the polymorphous transitions yielding α-Al_2O_3 come to the end, the granule strength increases independent of the initial phase composition of the alumina. The reason is that bulk sintering occurs at T>1200°C. According to the assumptions of Saalfeld [47], this sintering yields a coarsely disperse α-Al_2O_3 with primary particles larger than 700 Å. The strength of such particles and the area of contacts between them increase with sintering.

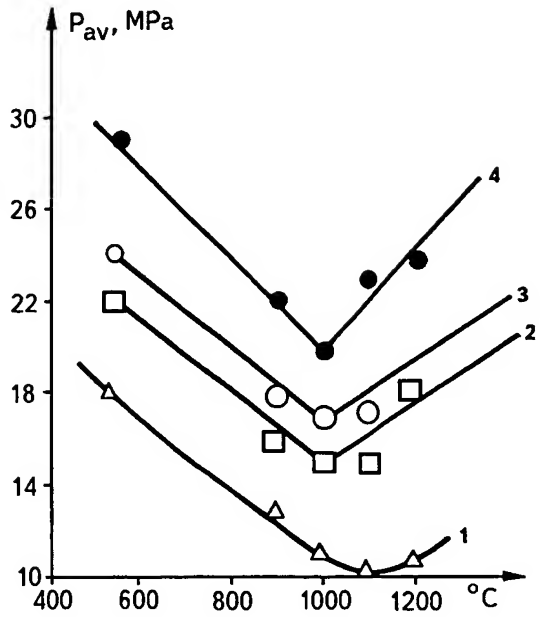

Fig. 9. Dependence of P_{av} on the calcination temperature for aluminas of different contents of χ-phase in samples after treatment at 550°C: (1) 50% χ-+50% γ-Al_2O_3; (2) 30% χ-+70% γ-Al_2O_3; (3) 20% χ-+80% γ-Al_2O_3; (4) 100% γ-Al_2O_3.

Similar results showing the effect of the calcination temperature on the alumina strength were reported in [50,51], and the reasons for such complicated temperature dependence of the strength of alumina granules obtained during calcination of γ-Al_2O_3 were discussed.

Therefore, we may focus on several important items concerning the thermal stability.

1. Stability of the low-temperature aluminas is determined by the set-on temperature of polymorphous transitions, i.e., the temperature at which the high-temperature modifications and α-Al_2O_3 appear.
2. Change of the specific surface related to the porous structure of the alumina may serve as an indirect characteristic of the thermal stability.
3. Mechanical strength is a key parameter determining the thermal stability of Al_2O_3.

As for spherical γ-Al_2O_3 used as the support for catalysts working in moving or fluidized beds, the

above results show that we managed to design the support with the best thermal stability and mechanical strength.

However, it is still necessary to improve these supports, since high-temperature processes, such as methane oxidation, combustion of off-gases, etc., impose more and more severe demands on supports and catalysts.

New approaches are required to solve this problem. Chemical modification of aluminum oxide/hydroxide by various dopings can be the way to improve the properties of the final product.

4. Alumina modification as a method to control its main properties

4.1. Modifiers and ways of their introduction

Modifiers can be divided into mineralizers and stabilizers according to their effect on materials (alumina in our case).

Mineralizers are substances that accelerate the changes of the basic material. For γ-Al_2O_3 these substances accelerate sintering and polymorphous transformations during the calcination lowering the temperature at which the high-temperature oxides and α-Al_2O_3 form. Oxides of copper [52,53], manganese [54–56], molybdenum and vanadium [55,56], fluorine and chlorine compounds [57], TiO_2 [55,58], etc. are among such substances.

Stabilizers are substances that decelerate the changes of the basic material. Zr and Y compounds [59–61], SiO_2 [62–65], and B_2O_5 [66–68] have such an influence on γ-Al_2O_3.

Besides, there are modifiers that improve the strength of alumina, such as compounds of Ba [69], B [67,68], Ca [70], and Mg [71,72]. Note, however, that data on the role of modifiers on alumina properties are contradicting.

We shall show below that this controversy about the role and mechanism of some additives is caused by the fact that different researchers use varying doping methods. The main differences lie in the

- dopant form (salt, hydroxide, oxide);
- introduction procedure (co-precipitation, alumina impregnation, hydroxide impregnation, oxide mixing, etc.);
- dopant amount;
- calcination conditions (rate of temperature rise, residence time at the given temperature, etc.);
- method of producing "pure" alumina and its properties.

In our research work we have stated and grounded main approaches to be used for alumina modification:

1. The most efficient dopes allowing the control of the alumina properties are: Mg – as a strengthening dope; La, Ce, Si as dopes improving the thermal stability.
2. In each metal/alumina system we verified the introduction method, the dope amount, the type of the low-temperature alumina, and the calcination conditions with regard to the properties of alumina obtained.
3. We have also designed special introduction procedures to obtain the optimum dope contents and studied the mechanisms of their modifying action.

Mg, La, Ce were introduced from the nitrate solutions, SiO_2 was introduced as the sol.

Let us now discuss the results obtained for each system. In all systems we studied two types of supports:

1. Spherical γ-Al_2O_3 (d=1.4–2.0 or 2.0–3.0 mm) prepared from commercial pseudoboehmite hydroxide.
2. Spherical γ-Al_2O_3 (d=1.4–2.0 or 2.0–3.0 mm) obtained via the TDP processing.

Spherical granules were produced using the HAM method.

4.2. Mg/Al_2O_3 system

Main results obtained with this system are reported in [73–80]. Mg was introduced from its aqueous nitrate solution either via incipient wetness impregnation of spherical γ-Al_2O_3 (two types) or by impregnating spherical granules of aluminum hydroxide precursors of oxides 1 and 2. We have designed an original impregnation procedure and apparatus, which are described elsewhere [73,75]. In [74] detailed studies of the Mg/alumina system have been published and the mechanism of the strengthening effect of Mg has been suggested. We have shown that only when

Mg^{2+} is introduced into aluminum hydroxide granules (independently of how the latter are prepared), Mg strengthens the γ-Al_2O_3 granules.

Summing up all the data we may draw the following conclusions:

1. Alumina strengthening occurs due to the formation of cation–anion solid solutions of Mg in alumina.
2. Such solid solutions form only from the solid solutions of pseudoboehmite structure when Mg is introduced into aluminum hydroxide.
3. Cation–anion solid solutions decrease the defectness of granules on a micron scale.

4.3. La/Al_2O_3 system

Results of a complex study of the effect of lanthanum cations on the thermal and mechanical stability (phase composition, mechanical strength, specific surface) of alumina depending on the introduction procedure and dope amount, calcination temperature and time are described in [81–84]. Even a small amount of the dope (up to 5% with La_2O_3) causes deceleration of the α-Al_2O_3 formation. At higher concentrations the transition of θ- to α-Al_2O_3 is completely suppressed and alumina is stabilized either in θ-form or in a mixture of γ- and δ-forms.

Therefore, it is possible to stabilize the transient forms of alumina up to 1200°C. Key factors determining the thermal stability of alumina in the La_2O_3–Al_2O_3 system are:

1. The effect of lanthana at the same introduction procedure is determined by the type of alumina used.
2. The introduction procedure of lanthana has a drastic effect on the change of the thermal stability. Thus, La introduction via the oxide granule impregnation (series I and II) is more efficient in comparison to the La salt introduction into AH granules.
3. There is an optimum amount of La for each introduction procedure and each type of initial γ-Al_2O_3 which completely suppresses the phase transitions in Al_2O_3.

The observed results allow us to conclude that the lanthana stabilizes the transition aluminas when a solid solution of La ions forms in the structure of the low-temperature aluminas. The presence of La in the alumina lattice prevents the diffusion of Al ions and the rearrangements into the high-temperature forms.

For convenience, in the next section we shall consider phase transitions observed in the Ce/Al_2O_3 system. Then in a separate section we shall unite the results concerning the main physical–chemical and structure–mechanical properties of alumina modified with La or Ce.

4.4. Ce/Al_2O_3 system

We performed our studies with the same samples of spherical aluminum hydroxide and oxide. We introduced Ce from its salts exactly as in the La/Al_2O_3 system, and we performed calcination in the same manner as well. The Ce content calculated as CeO_2 ranged from 1 to 13 wt% [85].

Like in the La_2O_3–Al_2O_3 system the strongest stabilization effect at the same way of Ce introduction was observed with the samples obtained from amorphous aluminum hydroxide (series II). This was proved by the largest absolute difference in the content of δ- and α-Al_2O_3 in these samples as compared to that of the pure support. The stabilizing effect is related to the stronger interaction of the dope with the alumina, as the latter contained χ-Al_2O_3 besides γ-Al_2O_3 due to peculiarities of its preparation. Most probably, not only γ-Al_2O_3, but also χ-Al_2O_3 interacts with Ce ions. The latter is more defective and disordered. That is why we observed no χ- and κ-Al_2O_3 at 550°C and 900°C, respectively, as in the La_2O_3–Al_2O_3 system (unlike in the non-doped aluminum of the series).

In comparison to the La_2O_3–Al_2O_3 system, CeO_2–Al_2O_3 never shows a phase in which Ce has reacted with Al_2O_3 in the X-ray patterns in the whole temperature range studied. Most likely, the Ce–Al_2O_3 system has two Ce-containing phases: (i) Ce oxide not interacting with alumina and imposing no stabilizing effect; (ii) highly disperse Ce compounds with alumina, which are not revealed in the X-ray patterns, but nevertheless affect the thermal stability of alumina. We failed to identify this phase. However, we believe in its existence judging from the fact that the intensities of CeO_2 profiles in mechanical mixtures and in our samples did not coincide at the same

concentration of Ce oxide. This assumption is confirmed by the X-ray studies performed on Pt–Ce–Al_2O_3 [86]. This paper discusses a highly disperse product forming at 550°C. This product results from the Ce interaction with the support and is Ce aluminate with a perovskite-like structure. This interaction is quite limited (not more than 5 mass% CeO_2 interacts with Al_2O_3).

Note that according to the data of other researchers [87], who used complex physical–chemical methods to study the thermal stability of alumina modified by Ce, the latter stays mainly as a disperse phase on the surface non-interacting with alumina. The authors of [87] explain this phenomenon by the fact that Ce has a weaker effect on the stability of alumina than La whose ions enter the alumina structure.

Thus, X-ray studies of two systems, La_2O_3–Al_2O_3 and CeO_2–Al_2O_3, prepared with the same alumina samples according to the same procedure and calcined at the same conditions allow us to conclude that alumina stabilization by Ce is weaker than by La. Such a behavior relates to the limited character of the interaction of ceria with the support.

4.5. *Structure and chemical properties of spherical alumina modified with La and Ce ions*

One of the publications [88] concerns the structural–mechanical properties of alumina modified by La and Ce ions.

4.5.1. *Specific surface area*

The specific surface area of doped aluminas was shown to be stabilized at temperatures ranging from 900°C to 1200°C. Thus at 1100°C the specific surface area of La-modified alumina was 3–6 times larger (depending on the alumina preparation procedure and dope amount) than that of "pure" alumina. The most pronounced stabilization effect was observed for samples containing 5% of La_2O_3. Therefore, the dope cation interacted actively with the support producing a solid solution with the structure of the corresponding alumina form.

The specific surface area of Ce-modified alumina exceeded that of "pure" alumina only by a factor of 1.2–2 upon calcination within the 900–1200°C range independent of the alumina preparation conditions.

Note that the stabilization effect on the BET surface area was more pronounced in the system La_2O_3–Al_2O_3 than in CeO_2–Al_2O_3 also at T>1200°C. The reason is the presence of lanthanum hexaaluminate, $La_2O_3 \cdot 11Al_2O_3$, whose concentration increases with the content of La_2O_3. Hexaaluminate is known [89] to have a layered structure that retains its large surface at high temperatures. In the CeO_2–Al_2O_3 system no cerium hexaaluminates were registered [90]. CeO_2 or Ce^{3+} compounds with alumina were coarsely disperse and had a small BET surface area [91].

4.5.2. *Pore structure*

We have studied the pore structure of samples for both doped and undoped alumina at 550°C and 1100°C. At 550°C the pore structure of modified samples practically did not differ from that of pure alumina. As the temperature increased, La- and Ce-modified samples behaved differently. Thus the pore volume (V_Σ) of CeO_2–Al_2O_3 practically did not change at 1100°C in comparison to that at 550°C as in pure alumina, whereas the average pore radius was 1.3 times smaller than for pure alumina.

In the La_2O_3–Al_2O_3 system V_Σ increased in comparison to that of non-modified alumina at 1100°C, the effective pore radius being three times less than for CeO_2–Al_2O_3. Therefore, sintering was certainly decelerated, and decelerated more efficiently for La_2O_3–Al_2O_3.

4.5.3. *Granule strength*

Since mechanical strength and mechanical stability are the main properties of the granular catalysts working in the fluidized bed (under local overheating), the effect of modifying dopes on the strength of alumina granules and the change of the sample strength in calcination was studied in [88].

Fig. 10 shows how the mechanical strength of granules (P_{av}) depends on the calcination temperature for "pure" alumina and for alumina doped by La and Ce. Apparently, at T>900°C all samples had the same mechanical strength. Raising the calcination temperature to 1100°C resulted in an increase of P_{av} for the "pure" alumina granules, which was very sharp for the samples containing 5 wt% of CeO_2. The strength of the samples containing 5 wt% of La_2O_3 increased only at T>1200°C. La-doped samples thus did not differ in this parameter from the "pure" alumina.

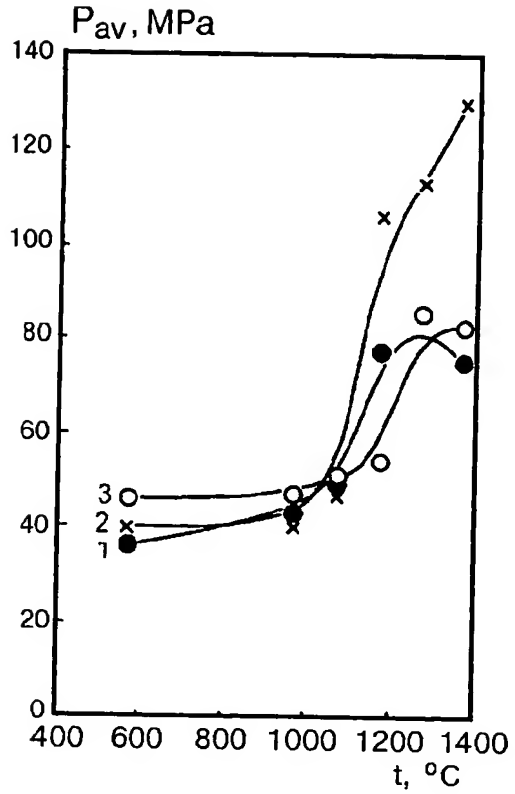

Fig. 10. Influence of calcination temperature on mechanical strength of alumina: 1 – pure Al_2O_3; 2 – 5% CeO_2/Al_2O_3; 3 – 5% La_2O_3/Al_2O_3.

Obviously, CeO_2 is a more efficient dope than La_2O_3 with regard to the mechanical strength. Most likely, the strength of modified samples changes with the transformation of the phase composition of these samples. According to the data obtained in [85], at T<900°C a highly disperse Ce-containing phase is present besides the Al_2O_3 and CeO_2 phases. It is not registered by the X-ray analysis due to the very low content. Since the mechanical strength of samples does not depend on the Ce content over the whole temperature range, we assume that the content of this X-ray amorphous phase is the same in all samples and does not depend on the concentration of CeO_2. Therefore, the strengthening is caused by an increase of the number of contacts, but by the strengthening of single contacts due to the interaction of the primary alumina particles with the dope.

For the La_2O_3–Al_2O_3 system [81] the low-temperature X-ray amorphous compound decomposes at T>1200°C producing α-Al_2O_3 and La hexaaluminate, thus not providing a high strength of the single contacts.

4.5.4. *Study of structural–mechanical properties of supports after calcination for prolonged periods of time*

In order to investigate how La–Al_2O_3 and Ce–Al_2O_3 behave during prolonged calcination at 1000°C, we have studied the change of S_{BET} for samples with the optimum dope content (5% of La_2O_3 or 2% of CeO_2). These data are shown in Fig. 11.

The sharpest change of S_{BET} occurred for all the samples during the first 5 h of calcination. A longer calcination decreased S_{BET} of non-modified samples, but not of the La-containing sample.

La-samples of alumina obtained from the gibbsite TDP (series 11) had the largest specific surface area after calcination for 30 h. For Ce-samples, stabilization of the surface area after 30 h calcination at 1000°C did not depend on the way of the alumina preparation.

S_{BET} dropped during calcination for a long period of time activation due to a change in the phase composition. δ-Al_2O_3 formed during the first hours of calcination at 1000°C, changing the particle morphology and package. As it is shown in [81,85], the pure oxide of the above spherical δ-Al_2O_3 support (1) had only the traces of α-Al_2O_3 after 2 h calcination, whereas there was up to 50% of α-Al_2O_3 in a differently prepared alumina sample, viz. the δ-Al_2O_3 support (2) produced via TPD processing. A longer calcination of pure alumina facilitates the phase transition to α-Al_2O_3 reducing S_{BET}. For some aluminas this transition was completed after calcination for 20 h. However, in other aluminas this transition was over already after 10 h. The content of the δ-phase grew with calcination time in all samples modified by La, but the traces of α-Al_2O_3 appeared only after 30 h. In the Ce-doped samples the δ-Al_2O_3 content also grew, but α-Al_2O_3 traces appeared after 20 h for one and after 10 h for another alumina. Meanwhile, the dispersity of CeO_2 particles did not increase.

Note that the modified samples did not lose their strength during a long time calcination at 1000°C, and were mechanically stable. The granule strength of La-doped samples of above δ-Al_2O_3 supports (1) and (2)

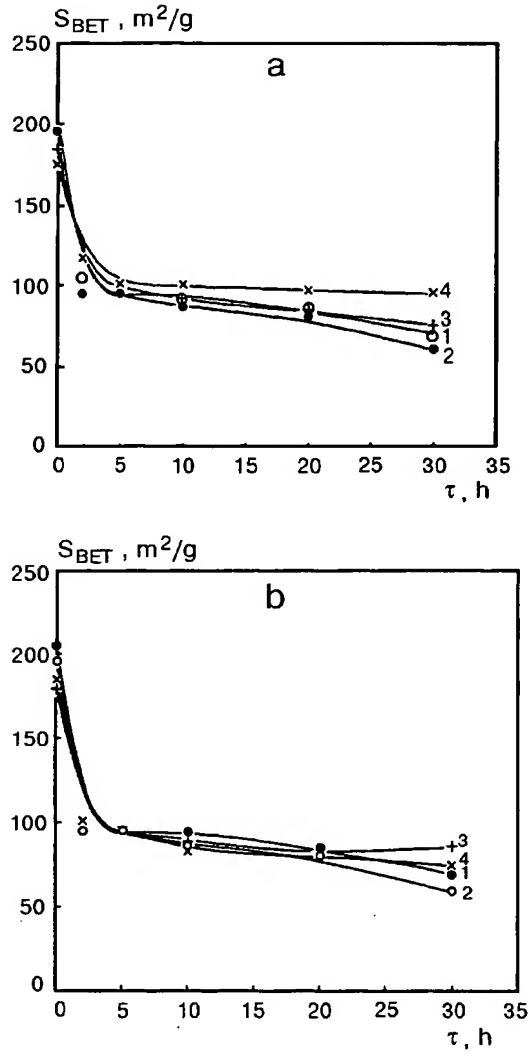

Fig. 11. Influence of calcination time at 1000°C on S_{BET} of alumina: (a) with 5% La_2O_3. 1 – Al_2O_3 support (1); 2 – Al_2O_3 support (2); 3 – La_2O_3/Al_2O_3 support (1); 4 – La_2O_3/Al_2O_3 support (2); (b) with 5% CeO_2. 1 – Al_2O_3 support (1); 2 – Al_2O_3 support (2); 3 – CeO_2/Al_2O_3 support (1); 4 – CeO_2/Al_2O_3 support (2). Support (1): spherical γ-Al_2O_3 prepared from commercial pseudoboehmite; support (2): spherical γ-Al_2O_3 produced by TDP processing.

after calcination for 30 h at 1000°C was 58.5 and 33 MPa, respectively. With the Ce-doped samples it was 54 and 30 MPa, respectively.

The results obtained agree well with our X-ray data on the La_2O_3–Al_2O_3 and CeO_2–Al_2O_3 systems. Thus La introduction into γ-Al_2O_3 produces a solid solution of La oxide based on the γ-Al_2O_3 structure where La ions substitute Al. This imposes limitations on the transitions to δ-, θ- and α-Al_2O_3. So, a large specific surface area is retained, and the mechanical properties of modified samples better resist high temperatures.

Unlike La_2O_3–Al_2O_3, alumina modified by CeO_2 does not show essential stabilization of the disperse structure of Al_2O_3. This is caused by the limitations on the interaction of alumina with Ce ions.

Therefore, modifying alumina with La and Ce ions, one can obtain alumina supports well resisting the effect of high temperatures.

4.6. *Alumina containing two dopes simultaneously*

Properties of alumina modified by the cations of two- or three-valent metals and interaction mechanisms discussed in Section 4.5.4 allow us to assume that introducing simultaneously two elements into alumina we may obtain a new family of supports exhibiting unique behavior. Moreover, studying such systems we may confirm or oppose our assumption on the mechanisms of the dope effects.

Below we shall consider the properties of alumina simultaneously containing Mg and La or Si and La dopes.

4.6.1. *Mg–La/Al_2O_3 system and its properties*

The X-ray studies show [81,84] that Mg and La ions present together in alumina improve its thermal stability, which is estimated from the content of α-Al_2O_3 formed at the given temperature, in comparison to the earlier studied La_2O_3–Al_2O_3 system.

Mg and La ions simultaneously present in alumina stabilize the solid solutions based on the γ-Al_2O_3 structure. The co-existence of Mg and La that favor to occupy different cation positions in the oxygen anion lattice in the γ-Al_2O_3-based solid solution does not allow the rearrangement of the solid solution structure typical for other ions. Moreover, the stabilized "rough" structure of the low-temperature solid solution facilitates the entrance of La into the support structure. Unlike the La_2O_3/Al_2O_3 system, here La ions diffuse mainly into the structure of solid mixed La–Mg/γ-Al_2O_3 at rising temperatures. If the solid La solution in alumina at T>1200°C yields $La_2O_3 \cdot 11Al_2O_3$, the solid La–Mg–γ-Al_2O_3 solution produces $2MgO–La_2O_3 \cdot 11Al_2O_3$. Both compounds

have a hexagonal packing of the oxygen lattice, as α-Al_2O_3, and are related, but have a higher symmetry.

Stabilization of Mg and La ions in the respective tetrahedral and octahedral positions hinders the Al ion diffusion yielding the high-temperature oxides. Calcination at 1400°C shows that it is necessary to optimize the ratio of Mg and La cations in the structure to stabilize the low-temperature solid solution. We may consider the mixed solution La–Mg–γ-Al_2O_3 with Mg:La∼1:1 as a low-temperature form of $2MgO–La_2O_3·11Al_2O_3$. To transit into the high-temperature form, this solid solution must be appropriately ordered with regard to the cation position occupation by La and Mg. According to the diffraction data, an La deficit yields a set of solid solutions or stoichiometric aluminum–magnesium spinel.

Therefore, the thermal stability of alumina simultaneously doped with two- and three-valent cations preferring to occupy different cation positions in the oxygen lattice of the low-temperature alumina results from the hindering of structure rearrangements in the structure of the mixed low-temperature solid solutions at increasing temperatures.

Structural–mechanical properties of alumina simultaneously doped with two- and three-valent cations have been studied in [84]. It was shown that the mechanical strength and thermal stability increased in this case.

4.6.2. *Mg–Ce/Al_2O_3 system*

As in the case of Mg–La/Al_2O_3, Mg was introduced into the spherical alumina hydroxide granules and cerium into γ-Al_2O_3 via incipient wetness impregnation with nitrate solutions. Sample properties were studied after calcination at 550–1300°C.

X-ray methods used to study the phase composition of alumina doped with Mg and Ce showed that Mg and Ce ions present in alumina did not increase its thermal stability in comparison to the CeO_2/Al_2O_3 and MgO–La_2O_3/γ-Al_2O_3 systems.

This effect is caused by the fact that only a small part of Ce introduced is able to interact with the support to stabilize as Ce^{3+} and slightly improve the thermal stability. The interaction product decomposes at higher temperatures, yielding a separate phase of cerium oxide, α-Al_2O_3 and a stoichiometric spinel. The major part of Ce introduced during impregnation transforms from Ce^{3+} to Ce^{4+} due to peculiarities of Ce chemistry to give the CeO_2 phase having no effect on the thermal stability of the support.

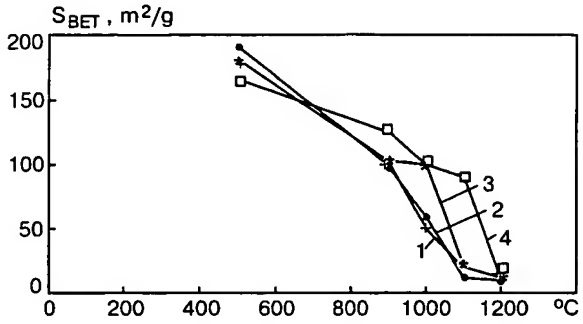

Fig. 12. Dependence of S_{BET} of alumina on temperature: 1 – pure Al_2O_3; 2 – 2.5% MgO/Al_2O_3; 3 – 5% CeO_2/Al_2O_3; 4 – Mg–Ce/Al_2O_3.

Note that unlike the system MgO–La_2O_3–Al_2O_3, $MgAl_{11}CeO_{19}$ (ASTM 26-879) was not formed here at T>1100°C. In the former system La almost completely interacts with the support yielding $MgAl_{22}LaO_{19}$ at the same temperatures.

Fig. 12 shows how the specific surface area of modified alumina changed with the calcination temperature. For comparison, we present data for "pure" alumina within the same figure (curve 1). Apparently, aluminas containing both Mg and Ce had the largest specific surface area at 900–1000°C. The specific surface area of the aluminas modified solely with Mg and of "pure" alumina, decreased in the above temperature range. Ce-doped alumina retained its surface up to 1100°C.

Fig. 13 and Table 4 show how the sample strength depended on the calcination temperature. Apparently, only the samples containing both Mg and Ce or Mg alone retained their high mechanical strength that even increased with temperature.

All the data obtained for the Mg–Ce/Al_2O_3 system prove that two- and three-valent cations both present in alumina enhance the effects of each other and allow one to improve the thermal and mechanical stability of alumina (though not so considerably as in Mg–La/Al_2O_3).

Therefore, only if a uniform solid mixed solution of ions forms in the low-temperature alumina, it is possible to obtain a support exhibiting high thermal stability. Moreover, the ions introduced must occupy respective tetrahedral or octahedral cation positions in the structure.

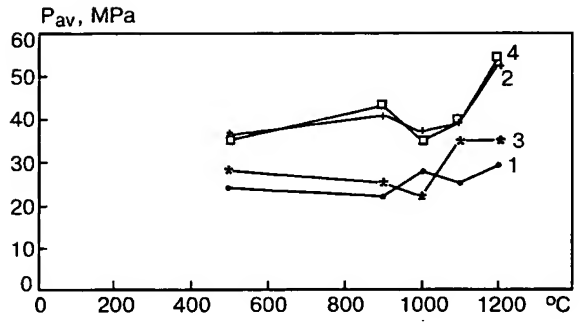

Fig. 13. Influence of calcination temperature on mechanical strength of alumina: 1 – pure Al_2O_3; 2 – 2.5% MgO/Al_2O_3; 3 – 5% CeO_2/Al_2O_3; 4 – Mg–Ce/Al_2O_3.

4.6.3. *La–Si/Al_2O_3 system*

It is known that SiO_2 introduced into alumina may substantially improve its thermal stability [63–66,92].

For us it was interesting to compare the SiO_2/Al_2O_3 system with Si–La/Al_2O_3. As shown in [83,93–95], introduction of SiO_2 (sol) into the plasticized paste of pseudoboehmite aluminum hydroxide obtained from TDP before molding allowed us to increase the thermal stability of alumina. So, S_{BET} of modified Al_2O_3 at 1200°C was 2.5 times higher than that of pure alumina.

Based on all our data, we have chosen the following composition to synthesize Si–La/Al_2O_3:

$$2.5\%\ SiO_2 + 5\%\ La_2O_3 + 92.5\%\ Al_2O_3$$

SiO_2 was introduced as a sol into the plasticized paste of TDP before HAM. Lanthanum was introduced into the spherical granules (diameter 2–3 mm) of γ-Al_2O_3 via incipient wetness impregnation with La nitrate solution. Then the granules were dried at 110°C and calcined at 550–1300°C (2 h at each temperature).

Table 4
Properties of spherical alumina

No.	Dope	S_{BET} (m^2/g)	Strength (MPa)	Phase composition
550°C				
1	–	200	24	γ-Al_2O_3
2	La	180	26	γ^*-Al_2O_3
3	Si	210	22	γ-Al_2O_3
4	Ce	185	21	γ-Al_2O_3+CeO_2
5	Mg	180	44	γ^*-Al_2O_3
6	La–Si	190	32	γ^*-Al_2O_3
7	La–Mg	160	38	γ^*-Al_2O_3
8	Ce–Mg	180	38	γ^*-Al_2O_3+CeO_2
1200°C				
1	–	7	28	α-Al_2O_3
2	La	29	35	$LaAlO_3$ (traces)+α-Al_2O_3+$La_2O_3 \cdot 11Al_2O_3$
3	Si	40	28	γ-Al_2O_3+40% α-Al_2O_3
4	Ce	14	35	α-Al_2O_3+CeO_2
5	Mg	10	60	$MgAl_2O_4$+α-Al_2O_3
6	La–Si	80	38	γ^*-Al_2O_3+δ-Al_2O_3 (~50%)
7	La–Mg	23	65	α-Al_2O_3+$MgAl_{11}LaO_{19}$+γ^{**}-Al_2O_3
8	Ce–Mg	23	60	$MgAl_2O_4$+α-Al_2O_3+CeO_2
1300°C				
1	–	6	30	α-Al_2O_3
2	La	28	44	α-Al_2O_3+La_2O_3+$La_2O_3 \cdot 11Al_2O_3$
3	Si	28	30	α-Al_2O_3
4	Ce	8	36	α-Al_2O_3+CeO_2
5	Mg	6	65	$MgAl_2O_4$+α-Al_2O_3
6	La–Si	26	48	α-Al_2O_3 (traces)+θ-Al_2O_3+$La_2O_3 \cdot 11Al_2O_3$ (traces)
7	La–Mg	14	70	α-Al_2O_3+$MgAl_{11}LaO_{19}$
8	Ce–Mg	10	65	$MgAl_2O_4$+α-Al_2O_3+CeO_2

γ^* – solid solution of Me cation on the base of γ-Al_2O_3.
γ^{**} – continuous number of low temperature solid solutions of La and Mg cations.

Table 4 shows the main properties of the system synthesized and compares it with "pure" alumina and alumina containing solely SiO_2 (2.5%) or La_2O_3 (5 wt%).

Apparently, La and Si both present in the system decelerated the phase transitions in alumina at rising temperatures. Thus the specific surface area remained large. The best stabilization effect was observed at T=1000°C. At 1100°C S_{BET} of the samples containing La–Si was twice higher than that of La/Al_2O_3 and Si/Al_2O_3. Calcination at 1300°C removed the difference between the S_{BET} of La/Al_2O_3, Si/Al_2O_3 and "pure" alumina, while the S_{BET} of $La–Si/Al_2O_3$ was 3–4 times higher. Note that the phase composition of these systems was considerably different. The α-Al_2O_3 phase appeared in $La–Si/Al_2O_3$ only at T=1300°C as traces. No lanthanum aluminate phase was registered in all high-temperature samples (T>1000°C) of the combined system. Lanthanum hexaaluminate appeared only at 1300°C. There were no other compounds indicating the interaction of La and Si oxides.

Note that the stabilization effect for the $La–Si/Al_2O_3$ system was far higher than that of $Mg–La/Al_2O_3$. Thus 15% of α-Al_2O_3 formed in $Mg–La/Al_2O_3$ after calcination at 1200°C (see Table 4), and S_{BET} of this sample was four times smaller than that of $La–Si/Al_2O_3$ containing no α-Al_2O_3 at this temperature. At 1300°C there was only α-Al_2O_3 in $Mg–La/Al_2O_3$ (5 wt% La_2O_3), whereas this phase was present only as traces in $La–Si/Al_2O_3$.

5. Conclusion

The data obtained in the fundamental studies allowed us to suggest a technological solution for the synthesis of spherical alumina with high mechanical strength and thermal stability.

Such alumina supports for catalysts operating in moving- or fluidized bed reactors can be prepared via the hydrocarbon–ammonia molding of pseudoboehmite aluminum hydroxide.

We suggested a new technology to produce pseudoboehmite aluminum hydroxide based on the thermal decomposition of gibbsite in the catalytic heat generator.

New spherical supports with unique properties were synthesized by modifying alumina with various dopes.

References

[1] B.C. Lippens, J.J. Steggerda, Physical and Chemical Aspects of Adsorbents and Catalysts, Academic Press, New York, 1970, p. 171.
[2] D.I. Trimm, A. Stanislaus, Appl. Catal. 21 (1986) 215.
[3] H.C. Stumpf, A.R. Russel, J.W. Newsome, C.M. Tucker, Ind. Eng. Chem. 45 (1953) 819.
[4] S.J. Wilson, J. Solid State Chem. 30 (1979) 247.
[5] T. Ono, Y. Ohguchi, O. Togari, in: G. Poncelet, P. Grange, P. Jacobs (Eds.), Preparation of Catalysis III, Elsevier, Amsterdam, 1983, p. 631.
[6] R.A. Shkrabina, Ph.D. Thesis, Institute of Catalysis, Novosibirsk, 1982 (in Russian).
[7] R.A. Shkrabina, Z.R. Ismagilov, M.N. Shepeleva et al., Proceedings of the 10th National Symposium on Catalysis Recent Development – Catalysis, Theory and Practicals, Madras, 18–21 December 1990, p. 30.
[8] G.K. Boreskov, E.A. Levitskii, Z.R. Ismagilov, J. Vses. obtsh. im Mendeleeva 29 (4) (1984) 379 (in Russian).
[9] Z.R. Ismagilov, M.A. Kerzhsenzev, J. Vses. obtsh. im Mendeleeva 35 (1) (1990) 43 (in Russian).
[10] Z.R. Ismagilov, M.A. Kerzhenzev, Catal. Rev.-Sci. Eng. 32 (1990) 51.
[11] Z.R. Ismagilov, R.A. Kerzhenzev, R.A. Shkrabina, Rus. Chim. J. 37 (1993) 48 (in Russian).
[12] Z.R. Ismagilov, R.A. Shkrabina, M.A. Kerzhenzev, G.B. Barannik, React. Kinet. Catal. Lett. 55(2) (1995) 489.
[13] Ya.Z. Kazobashvili, G.M. Micheev, Neftepererabotka neftechim., Moscow 12 (1964) 11 (in Russian).
[14] V.A. Dzisko, A.P. Karnaukhov, D.V. Tarasova, Physicochemical Basis of Oxide Catalysts Synthesis, Nauka, Novosibirsk, 1978, p. 300 (in Russian).
[15] V.V. Plaksina, Yu.N. Fomichev, M.E. Levinter, in: R.A. Buyanov (Ed.), Scientific Basis of Catalysts Preparation, Institute of Catalysis, Novosibirsk, 1983, p. 216 (in Russian).
[16] G.M. Gusev, L.G. Shumskaya, N.M. Lyamina, Dokl. AN SSSR 235 (1977) 921 (in Russian).
[17] S.M. Paramzin, Yu.D. Pankratiev, O.P. Krivoruchko et al., Izv. SO AN SSSR, Ser. Chim. 4 (1984) 33 (in Russian).
[18] Rhone Poulenc, Eur. Patent N 55164 (1981).
[19] Leuna Werke, Patent DDR N 203 038 (1983).
[20] R.A. Shkrabina, E.M. Moroz, E.A. Levitskii et al., Kinet Katal. 22 (1981) 1603 (in Russian).
[21] Yu.K. Vorobiev, R.A. Shkrabina, E.A. Levitskii, Kinet. Katal. 22 (1981) 1595 (in Russian).
[22] M.N. Shepeleva, R.A. Shkrabina, V.B. Fenelonov, Z.R. Ismagilov, Appl. Catal. 78 (1991) 175.
[23] M.N. Shepeleva, V.B. Fenelonov, R.A. Shkrabina, E.M. Moroz, Kinet. Katal. 27 (1986) 1202 (in Russian).
[24] M.N. Shepeleva, R.A. Shkrabina, L.G. Okkel et al., Kinet. Katal. 29 (1988) 195 (in Russian).
[25] P.V. Klassen, I.G. Grishaev, The Basis of Granulation Methods, Chimiya, Moscow, 1982 (in Russian).
[26] H. Shubert, Chem. Ing. Thechnol. 47 (1975) 86.
[27] C. Perego, P.L. Villa, Proceedings of the Third Seminar of Catalysis, Rimini, Chapter 2, 19–24 June 1994, Italy, p. 25.

[28] Rhone Poulenc, US Patent 4 273 620 (1965).
[29] Labofina French Patent 2 261 056 (1975); 2 261 057 (1975).
[30] M.N. Shepeleva, R.A. Shkrabina, Z.R. Ismagilov, Technol. Today 3 (1990) 150.
[31] M.N. Shepeleva, R.A. Shkrabina, Z.R. Ismagilov, V.B. Fenelonov, in: G. Poncelet, P.A. Jacobs, B. Delmon (Eds.), Proceedings of the Fifth Symposium on Preparation of Catalysts, Elsevier, Amsterdam, 1991, p. 583.
[32] Z.R. Ismagilov, M.N. Shepeleva, R.A. Shkrabina, V.B. Fenelonov, Appl. Catal. 69 (1991) 65.
[33] M.N. Shepeleva, R.A. Shkrabina, Z.R. Ismagilov et al., Kinet. Katal. 32 (1991) 132 (in Russian).
[34] R.A. Rebinder, E.D. Shchukin, L.Ya. Margolis, Dokl. AN SSSR 154 (1964) 695 (in Russian).
[35] L.Ph. Melgunova, Z.R. Ismagilov, R.A. Shkrabina, Proceedings of the European Congress on Catalysis, vol. 1, (EUROPACAT-1): Book of Abstracts V.2.-Montpellier, France, 2–3 September 1993, p. 992.
[36] Z.R. Ismagilov, M.N. Shepeleva, R.A. Shkrabina et al., Proceedings of the Workshop on The Problems of Strength of Granulated Supports and Catalysts, Novosibirsk, 10–13 October 1987, p. 40 (in Russian).
[37] R.A. Rebinder, Physico-chemical Mechanics of Dispersed Materials, Nauka, Moscow, 1966 (in Russian).
[38] E.D. Schukin, A.Yu. Bessonov, S.A. Paranskii, Mechanical Testing of Catalysts and Sorbents, Nauka, Moscow, 1971, p. 115 (in Russian).
[39] D.I. Titelman, A.P. Shlakov, A.I. Kruindel, N.A. Karabajyan, Metody Analiza i Kontrolja 5 (1983) 34 (in Russian).
[40] L.V. Kovalskaya, Ph.D. Thesis, Grozny, 1983 (in Russian).
[41] E.G. Avvakumov, Mechanical Methods of Chemical Processes Activation, Nauka, Novosibirsk, 1986 (in Russian).
[42] N.V. Perzev, Ph.B. Danilova, V.G. Babak et al., Dokl. AN SSSR 222 (1975) 1085 (in Russian).
[43] I.A. Stepanov, Izv. AN Latv. SSR. Ser. Phys. i Tech. Nauk. 2 (1985) 83 (in Russian).
[44] M.N. Shepeleva, Z.R. Ismagilov, R.A. Shkrabina, I.A. Ovsyannikova, Kinet. Katal. 32 (1991) 455 (in Russian).
[45] Z.R. Ismagilov, N.A. Koryabkina, I.A. Ovsyannikova, R.A. Shkrabina, Kinet. Katal. 32 (1991) 494 (in Russian).
[46] I.A. Ovsyannikova, G.I. Goldenberg, N.A. Koryabkina, R.A. Shkrabina, Z.R. Ismagilov, Appl. Catal. 55 (1989) 75.
[47] H. Saalfeld, Neues Jahrb. Mineral Abhanell. 95 (1960) 1.
[48] Z.R. Ismagilov, R.A. Shkrabina, M.N. Shepeleva, N.A. Koryabkina, Proceedings of the Second All-Union Workshop on Catalyst Deactivation, Ufa, 10–13 May 1989, p. 111 (in Russian).
[49] V.N. Kuklina, L.M. Plyasova, L.M. Kepheli, E.A. Levitskii, Kinet. Katal. 12 (1971) 1078 (in Russian).
[50] B.M. Phedorov, V.M. Balashov, A.S. Berenblyum, Kinet. Katal. 31 (1990) 673 (in Russian).
[51] B.M. Phedorov, V.I. Nechoroshev, I.A. Zhukov, A.S. Berenblyum, Kinet. Katal. 32 (1992) 190 (in Russian).
[52] E.M. Moroz, O.A. Kirichenko, V.A. Ushakov, E.A. Levitskii, React. Kinet. Catal. Lett. 28 (1985) 9.
[53] O.A. Kirichenko, V.A. Ushakov, E.M. Moroz, Z.R. Ismagilov, React. Kinet. Catal. Lett. 38 (1989) 307.
[54] P.G. Tsyrulnikov, V.S. Salnikov, A.S. Noskov, Proceedings of the 11th International Conference on Modern Trends in Chemical Kinetics and Catalysis, Novosibirsk, Part 2, 13–15 November 1995, p. 402.
[55] K. Gauguin, M. Granulier, D. Papee, Catalysis for Control of Automobile Pollution, Washington, 1975, p. 147.
[56] B.S. Porekh, S.W. Weller, J. Catal. 55 (1978) 58.
[57] T.V. Antipina, V.V. Yuschenko, J. Phys. Chem. 50 (1976) 2921 (in Russian).
[58] H. Sabiro, I. Yoshio, Y. Masahiro, S. Shigeyuki, J. Ceram. Soc. Jpn. 94 (1986) 400.
[59] M. Johnson, J. Catal. 123 (1990) 245.
[60] Patent USA 4 708 946 (1987).
[61] K. Akita, Y. Hisao, M. Shimplei, Proceedings of the Eighth Jap–USSR Catalysis Seminar, Tokyo, 29–31 October 1986, p. 24.
[62] C. Thierry, L. Jean-Luc, Patent France 2 697 832 (1994).
[63] M.N. Shepeleva, B.R. Bunimovich, O.A. Kirichenko et al., in: A. Samachov (Ed.), Scientific Bases of Catalyst Preparation, Institute of Catalysis, Novosibirsk, 1983, p. 234 (in Russian).
[64] R.K. Iler, J. Am. Cer. Soc. 47 (1964) 339.
[65] E. Yoldas Bulent, J. Mater. Sci. 11 (1976) 465.
[66] Patent USA 3 956 186 (1976).
[67] N.F. Ermolenko, M.D. Efros, Vesti AN BSSR, Ser. Chim. Nauk. 3 (1973) 5 (in Russian).
[68] V.A. Peregudov, N.V. Kochetkova, E.V. Gorotshankin, V.N. Anochin, Proceedings of the Nauchno-techn. Conference, Moscow Chim. Techn. Institute (branch), Novomoskovsk, part 2, 6–11 February 1984, p. 8 (in Russian).
[69] M. Masato, E. Koichi, A. Himomichi, J. Chem. Lett. 2 (1986) 151.
[70] V.L. Ermak, T.L. Pashkova, G.M. Belotserkovskii, I.Ya. Tyuryaev, Catalysts of Basic Organic Synthesis, Leningrad, 1973, N. 68, p. 77 (in Russian).
[71] D.K. Nukherjee, B.N. Samaddar, J. Trans. Indian. Ceram. Soc. 48 (1989) 23, 35.
[72] A.W. Kaysser, M. Sprissler, C.A. Handwerker, J.E. Blendell, J. Am. Ceram. Soc. 70 (1987) 339.
[73] Russian Patent Appl. N94 007 256, pr.15.03.94.
[74] N.A. Koryabkina, Ph.D. Thesis, Institute of Catalysis, Novosibirsk, 1993 (in Russian).
[75] Pat. Rus. Fed. 1 660 276, 25.08.1989.
[76] N.A. Koryabkina, G.S. Litvak, R.A. Shkrabina, Z.R. Ismagilov, Kinet. Katal. 34 (1993) 913 (in Russian).
[77] N.A. Koryabkina, Z.R. Ismagilov, R.A. Shkrabina, E.M. Moroz, V.A. Ushakov, Appl. Catal. 72 (1991) 63.
[78] N.A. Koryabkina, Z.R. Ismagilov, R.A. Shkrabina, E.M. Moroz, V.A. Ushakov, Kinet. Katal. 32 (1991) 1013 (in Russian).
[79] Z.R. Ismagilov, N.A. Koryabkina, N.A. Rudina, G.I. Goldenberg, I.A. Ovsyannikova, R.A. Shkrabina, Kinet. Katal. 32 (1991) 494 (in Russian).
[80] I.A. Ovsyannikova, G.I. Goldenberg, N.A. Koryabkina, R.A. Shkrabina, Z.R. Ismagilov, Appl. Catal. 55 (1989) 75.
[81] R.A. Shkrabina, N.A. Koryabkina, V.A. Ushakov, E.M. Moroz, M. Lausberg, Z.R. Ismagilov, Kinet. Katal. 37 (1996) 116 (in Russian).

[82] Z.R. Ismagilov, R.A. Shkrabina, N.A. Koryabkina, V.A. Ushakov, Kinet. Katal., 38, N1 (1997) 133 (in Russian).
[83] Z.R. Ismagilov, R.A. Shkrabina, N.A. Koryabkina, F. Kapteijn, Catal. Today 24 (1995) 269.
[84] N.A. Koryabkina, R.A. Shkrabina, V.A. Ushakov, Z.R. Ismagilov, Catal. Today 29 (1996) 427.
[85] N.A. Koryabkina, R.A. Shkrabina, V.A. Ushakov, E.M. Moroz, M. Lausberg, Z.R. Ismagilov, Kinet. Katal. 37 (1996) 124 (in Russian).
[86] V.A. Drozdov, P.G. Tsirulnikov, V.V. Popovskii et al., Kinet. Katal. 27 (1986) 721 (in Russian).
[87] M. Ozava, M. Kimura, A. Isogai, J. Les Common Met. 162 (1990) 297.
[88] R.A. Shkrabina, N.A. Koryabkina, V.A. Ushakov, M. Lausberg, Z.R. Ismagilov, F> KapteijnKinet. Katal., 38, N1 (1997) 128 (in Russian).
[89] J.L. Duplan, H. Praliaud, Appl. Catal. 67 (1991) 325.
[90] H. Yamashita, A. Kato, N. Watanad, S. Matsuda, Nippon Kagaki Kaishi (1986) 1169.
[91] A.B. Kiss, G. Keresztur, L. Farkas, Spectrochim. Acta 36 (1980) 653.
[92] B. Beguin, E. Gazbowski, M. Primet, J. Catal. 127 (1991) 595.
[93] R.A. Shkrabina, N.A. Koryabkina, Z.R. Ismagilov, V.A. Ushakov, L.T. Tsykoza, D.A. Arendarskii, Proceedings of the Seventh Nordic Symposium Catalysis, Book of Abstracts, Turku, Finland, 2–4 June 1996, p. 31.
[94] Z.R. Ismagilov, R.A. Shkrabina, N.A. Koryabkina, Proceedings of the 11th International Congress on Catalysis – 40th Anniversary, Baltimore, USA, 30 June–5 July 1996, p. 100.
[95] N.A. Koryabkina, R.A. Shkzabina, Z.R. Jsmagilov, Proceedings of conference "The problems of Catalyst Deactivations", Ufa, (1989), Part I, 18 (in Russian)..